Solvent Effect on the Decarbonylation of Acyl Radicals Studied by Laser Flash Photolysis

Yuri P. Tsentalovich and Hanns Fischer
Physikalisch-Chemisches Institut det Universität Zürich, Winterthurerstrasse 190, CH-8057, Switzerland

Absorption spectra of transient radicals generated from dibenzyl and di-*tert*-butyl ketones and rate constants for their fragmentation and termination reactions were obtained by laser flash photolysis in various solvents. Whereas the pivaloyl radical absorbs only for $\lambda \leqslant 240$ nm, the first absorption band of phenylacetyl is red shifted which is ascribed to a phenyl–carbonyl conjugation. The rate constant for the decarbonylation of the acyl radicals decreases markedly with increasing solvent polarity. This is explained by the dipole moment which decreases during the scission process.

The photolyses of di-*tert*-butyl and dibenzyl ketones are classical Type I cleavage reactions[1–4] and follow a particularly clean reaction Scheme (1)–(6). Therefore, they have been widely

$$\text{R–CO–R} \xrightarrow{h\nu} \text{R–CO–R}(S_1) \xrightarrow{<10^{-8}\ \text{s}} \text{R–CO–R}(T_1) \quad (1)$$

$$\text{R–CO–R}(T_1) \xrightarrow{<10^{-9}\ \text{s}} \text{R–}\dot{\text{C}}\text{O} + \dot{\text{R}} \longrightarrow \text{Geminate products + Free radicals} \quad (2)$$

$$\text{R–CO} \xrightarrow{k_{CO}} \dot{\text{R}} + \text{CO} \quad (3)$$

$$2\text{R–}\dot{\text{C}}\text{O} \xrightarrow{2k_1} \text{Products} \quad (4)$$

$$2\dot{\text{R}} \xrightarrow{2k_2} \text{Products} \quad (5)$$

$$\text{R–CO} + \dot{\text{R}} \xrightarrow{k_x} \text{Products} \quad (6)$$

used to test experimental techniques for detection of transient radicals in liquid solution, such as EPR,[5] optical[6–10] and IR spectroscopy,[11] CIDNP,[12,13] CIDEP[14] and polarimetry.[15] They were also employed as bases for quantitative studies of nuclear[16] and electron spin polarization,[17,18] of magnetic field and isotope effects on reaction yields,[19,21] on the reaction dynamics in restricted environments[22] and of the kinetics of radical self-terminations,[23] radical–molecule reactions[24] and radical fragmentations.[6,7,23,25] Besides the general Scheme (1)–(6) many mechanistic and kinetic details were well established in these studies.

Here we use the ketones again to test a newly constructed and in part unconventional laser flash photolysis arrangement and add to the understanding of the reactions by the detection of optical spectra of the acyl radicals R–$\dot{\text{C}}$O and of a rather pronounced solvent effect on their decarbonylation (3). The latter effect is discussed in terms of a lower dipolar stabilization of the transition state as compared with the parent radicals. We also report absorption coefficients and self-termination rate constants for benzyl and *tert*-butyl radicals which confirm previous data.

Experimental

Fig. 1 shows a schematic representation of the experimental arrangement which is similar to previously described systems.[26–28] The radiation from a Lambda Physik LPX 100 excimer laser (308 nm, maximum pulse energy 100 mJ) is concentrated *via* spherical and cylindrical lenses, calibrated glass filters F3 for intensity reduction and a shutter S2 to a Suprasil cell with 3 × 10 × 50 mm^3 inside dimension and has an area of 9 × 11 mm^2 at the cell front. The sample solutions flow through the cell with a rate of 3 cm^3 min^{-1} which replaces the solution in the photolysis region after an average of 1–2 pulses.

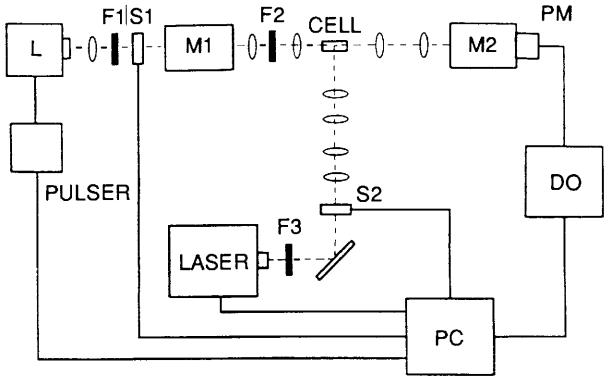

Fig. 1 Scheme of the experimental arrangement (see text for symbols)

The monitoring system consists of a 450 W xenon short-arc lamp (Osram XBO 450 W/4) pulsed with 100–250 A for 2 ms, two synchronously operating monochromators M1 and M2, a water (F1) and a neutral density (F2) filter, and a Hamamatsu R955 photomultiplier. M1 is a Bausch & Lomb high intensity monochromator (1350 grooves/mm, bandwidth 10 nm), M2 was home-built (1200 grooves/mm, bandwidth 5 nm). The use of two monochromators allows one to avoid depletion of the solution by the monitoring light completely and increases the spectral selectivity of the system. The photomultiplier usually operated with 1000 V total and four dynodes. Between the last amplification stages large capacitors were inserted to hold the voltage distribution constant during the detection pulses. The remaining small non-linearity of the response was taken into account in determinations of absorption coefficients but did not disturb the kinetic traces since the transient signals were small compared to the total incident light intensity. The monitoring beam has dimensions of 2.5 × 8 mm^2 at the edges and 2 × 7 mm^2 at the centre of the cell. The total spectral range is 220–800 nm.

The photomultiplier signal is measured over a 50 Ω resistor by a LeCroy 9400 digital oscilloscope. To obtain one kinetic

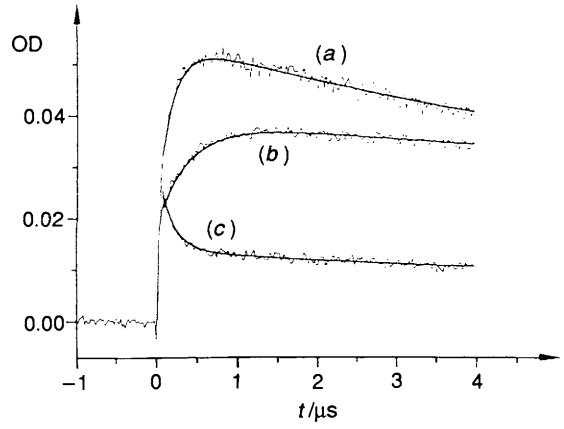

Fig. 2 Transient absorption kinetics of benzyl radicals (317 nm) in (*a*) hexane and (*b*) methanol and of phenylacetyl and benzyl radical (275 nm) in (*c*) hexane

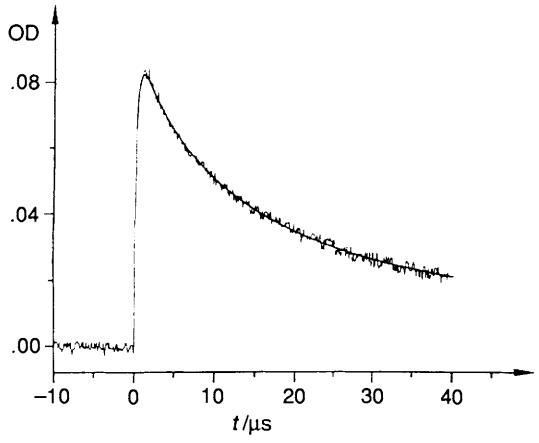

Fig. 3 Transient absorption kinetics of benzyl radicals (317 nm) in methanol for an extended time period

trace 10–50 signals following properly timed laser-lamp pulse sequences were averaged for each of the three shutter configurations $\overline{S}1S\overline{2}$ (background), $\overline{S}1S2$ (fluorescence) and S1S2, transferred to a PC and then combined to correct for background and fluorescence. The PC also controls the operation of the laser, the lamp pulser and shutters *via* an IEEE interface MP488CT. Triggering of the oscilloscope was synchronized with the laser pulse using a photodiode. The laser output was permanently monitored by a Gentec ED-500 joulemeter and was found constant within about 20%.

Typically, the optical densities of the ketone solutions in the 3 mm cell were 0.05–0.08 at 308 nm. This ensured a fairly homogeneous radical production and suggests that the initial radical concentrations are given by eqn. (7). Here, E_L is the laser

$$[\dot{R}]_0 = [R\dot{C}O]_0 = \frac{E_L \times \Phi}{h\nu \times N_A \times V}(1 - 10^{-OD}) \quad (7)$$

pulse energy incident on the cell, Φ is the quantum yield of the cleavage (1,2), OD is optical density of the ketone solution along the 2 mm width of the detection beam, and $V = 9 \times 11 \times 2$ mm^3 follows from the beam dimensions. To test eqn. (7), kinetic experiments were performed with di-*tert*-butyl ketone in tetradecane for which $\Phi = 0.72$ and the self-termination rate constant for *tert*-butyl radicals at room temperature $2k_t = 3.4 \times 10^9$ dm^3 mol^{-1} s^{-1} are well established.[29] Using these values the initial radical concentration was obtained from fits to the second order decay of *tert*-butyl at long times and was found 30% lower than calculated *via*

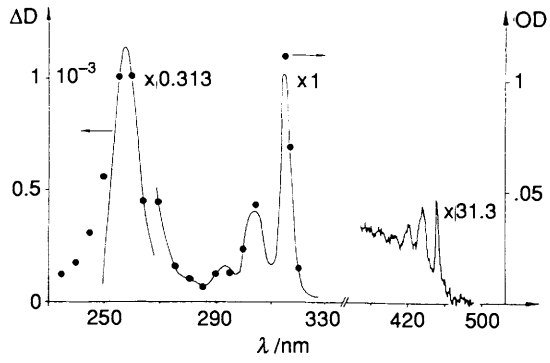

Fig. 4 Absorption spectrum of the benzyl radical: dots, this work, solvent hexane; solid line, ref. 8, solvent cyclohexane

eqn. (7). Assuming that the same deviation holds for all other experiments eqn. (7) was then used throughout this work but corrected correspondingly.

Tetradecane was purified by chromatography, and all other chemicals were applied in the purest commercially available forms. Solutions were freed from oxygen prior to use by purging with helium for at least one hour. All data given below refer to room temperature (23 ± 1) °C.

Results

Dibenzyl Ketone.—The traces (*a*) and (*b*) of Fig. 2 were obtained at the 317 nm absorption maximum of the benzyl radical after pulse photolysis of 10^{-3} mol dm^{-3} dibenzyl ketone in hexane (*a*) and in methanol (*b*). They are very similar to those reported by Scaiano *et al.*[6] and by Turro *et al.*[7] and correspond to the expected sequence of benzyl formation: an initial nanosecond rise of the absorption by the rapid reactions (1) and (2) is followed by a slower increase which reflects the decarbonylation (3) of the phenylacetyl radical. A comparison of the traces (*a*) and (*b*) reveals that the decarbonylation is slower for the solvent methanol. At the end of the traces the benzyl radicals start to decay by second-order self-termination. This is more clearly seen on the extended time scale of Fig. 3. Trace (*c*) of Fig. 2 shows the transient absorption for the same photolysis but observed at 275 nm. Now, the initial jump is followed by a fast decay which corresponds to the growth in trace (*a*) and which is attributed to the absorption of the phenylacetyl radical. This had not been detected before.

Fig. 4 shows an absorption spectrum taken point by point for a time-delay of 600 ns after the photolysis pulse for which the decarbonylation is nearly complete. It depends little on the solvent and coincides with a spectrum of the benzyl radical measured by modulation spectroscopy[8] (solid line). A spectrum taken at 80 ns delay, *i.e.* at the on-set of the decarbonylation also coincided with the spectrum of benzyl for $\lambda \geqslant 300$ nm but showed marked deviations at lower wavelengths. The differences are assigned to the phenylacetyl radical absorption and are shown in Fig. 5. We were not able to obtain it for $\lambda < 270$ nm, *i.e.* within strong 260 nm band of benzyl,[8] and conclude that the absorption coefficient of the acyl radical is much smaller than that of benzyl in the low wavelength region.

For quantitative analyses kinetic measurements were carried out for $\lambda = 317$ and 275 nm, seven solvents and different time scales. Moreover, for each solvent three different incident laser energies were used which lead to different initial radical concentrations in the range $2.7 \times 10^{-6} \leqslant [\dot{R}]_0 \leqslant 1.5 \cdot 10^{-5}$ mol dm^{-3}. Since the absorption coefficient of the ketone varied slightly with the solvents the ketone concentration was adjusted to maintain a constant OD = 0.16 for a 1 cm cell.

Table 1 Decadic absorption coefficients and rate constants for benzyl (R) and phenylacetyl (RCO) radicals

Solvent	ε_R(317 nm)/ dm^3 mol^{-1} cm^{-1}	ε_R(275 nm)/ dm^3 mol^{-1} cm^{-1}	ε_{RCO}(275 nm)/ dm^3 mol^{-1} cm^{-1}	k_{CO}/s^{-1}	$2k_t$/dm^3 mol^{-1} s^{-1}
Cyclohexane	8500	700	2200	$6.0 \cdot 10^6$	4.2×10^9
Hexane	7700	700	2300	$5.3 \cdot 10^6$	9.1×10^9
Tetradecane	8600	800	—	—	3.0×10^9
Propan-2-ol	6100	600	2000	$3.1 \cdot 10^6$	3.2×10^9
Ethanol	6500	700	2100	$2.8 \cdot 10^6$	3.9×10^9
Methanol	6500	600	2000	$2.5 \cdot 10^6$	5.6×10^9
Acetonitrile	7500	800	2300	$1.7 \cdot 10^6$	6.3×10^9

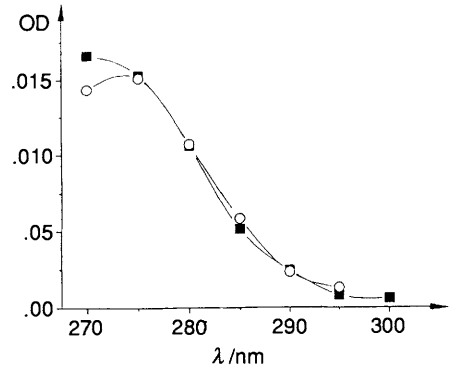

Fig. 5 Absorption spectrum of the phenylacetyl radical: circles, solvent hexane; squares, solvent methanol

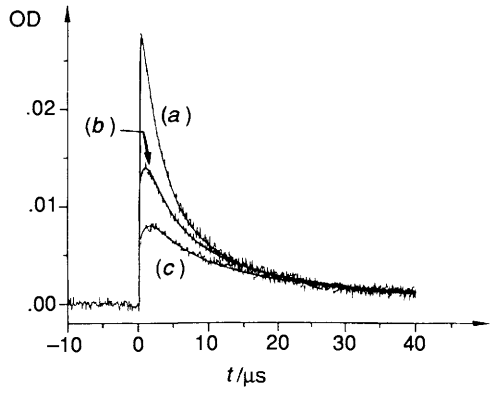

Fig. 6 Transient absorption kinetics of the *tert*-butyl radical (317 nm) in hexane for different photolysis pulse energies (*a*)–(*c*).

Reactions (3) to (6) have the kinetic eqns. (8) and (9) and the

$$\frac{d[R\dot{C}O]}{dt} = -k_{CO}[R\dot{C}O] - 2k_t[R\dot{C}O]^2 - 2k_x[R\dot{C}O][\dot{R}] \quad (8)$$

$$\frac{d[\dot{R}]}{dt} = k_{CO}[R\dot{C}O] - 2k_2[\dot{R}]^2 - 2k_x[R\dot{C}O][\dot{R}] \quad (9)$$

initial condition $[R\dot{C}O]_0 = [\dot{R}]_0$. The radical concentrations are linearly related to the optical densities *via e.g.* $OD(\dot{R}) = \varepsilon_R[\dot{R}]L = -\log(1 - I_R/I_0)$ where I_0 is the photomultiplier signal in the absence of transients, and I_R is the transient signal; $L = 1$ cm is the pathlength of the monitoring beam.

To extract the relevant parameters by fits of eqns. (7)–(9) to the kinetics traces we use the common approximation $2k_1 = 2k_2 = k_x = 2k_t$ which is normally allowed for diffusion controlled terminations of similarly sized radicals,[23] and assume that the quantum yield of radical formation is equal to $\Phi = 0.7$

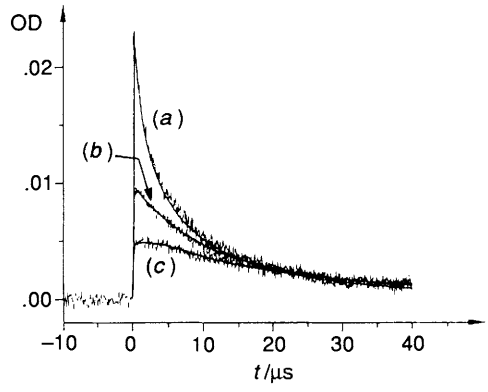

Fig. 7 Transient absorption kinetics of the *tert*-butyl radical (317 nm) in acetonitrile for different photolysis pulse energies (*a*)–(*c*).

for all solvents.[2,3] For the 317 nm traces the values of k_{CO}, $2k_t$ and the absorption coefficient of benzyl ε_R were treated as free parameters whereas the initial radical concentrations were estimated as described above. The traces obtained at 275 nm were then analyzed with k_{CO} and $2k_t$ fixed and the absorption coefficients of phenylacetyl and benzyl as free parameters. For tetradecane solvent the initial parts of the traces were disturbed by a longer lived fluorescence of unknown origin which precluded the determination of k_{CO} and of ε_{RCO}. The curves drawn in Figs. 2 and 3 show some results of the fitting procedures, and the numerical values of the parameters are collected in Table 1. We estimate the errors of the data to ± 20%.

Di-tert-*butyl Ketone*.—Figs. 6 and 7 show transient optical traces obtained at the absorption maximum of the *tert*-butyl radical $\lambda = 315$ nm during photolysis of 1.45×10^{-2} mol dm^{-3} di-*tert*-butyl ketone in hexane and in acetonitrile for three different initial radical concentrations. For the lower radical concentrations (*b*,*c*) the initial rises due to decarbonylation of the pivaloyl radical (3) are observed again but they are less pronounced and slower than for phenylacetyl (Figs. 2 and 3). Therefore, the decarbonylation and self-termination reactions are not separated in time, here. For acetonitrile the decarbonylation is hardly resolved because it is even slower than in hexane.

A transient absorption spectrum was recorded for hexane solvent immediately after the photolysis pulse and is displayed in Fig. 8 together with the spectrum of the *tert*-butyl radical measured by modulation spectroscopy in heptane.[9] For $\lambda \geqslant 240$ nm the spectrum is obviously solely due to *tert*-butyl but at shorter wavelength there are deviations which we ascribe to the pivaloyl radical. This is supported by kinetic traces recorded for $\lambda \leqslant 240$ nm which did not show any indication for the decarbonylation process as expected if *tert*-butyl and pivaloyl both contribute with similar absorptions.

As for dibenzyl ketone the kinetic data obtained at 315 nm

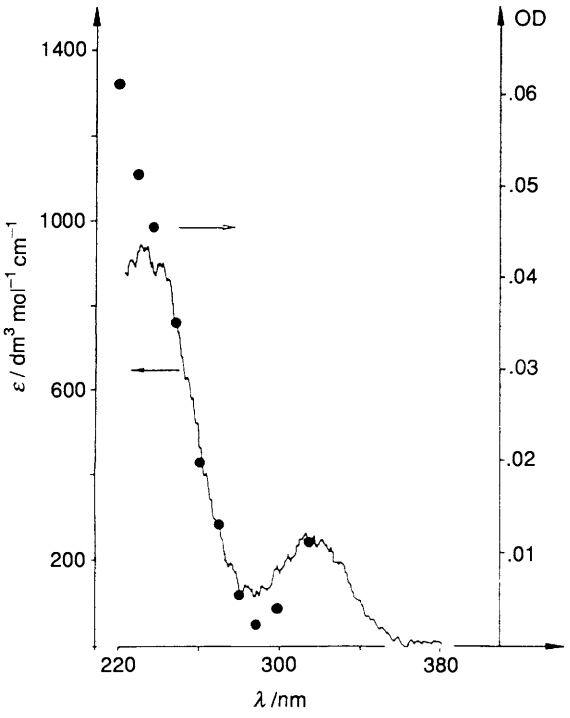

Fig. 8 Transient absorption (dots) 1 μs after pulse photolysis of di-*tert*-butyl ketone in hexane: solid line, absorption spectrum of the *tert*-butyl radical[9]

Table 2 Decadic absorption coefficients and rate constants for *tert*-butyl (R) and pivaloyl (RCO) radicals

Solvent	ε_R(315 nm)/ dm³ mol⁻¹ cm⁻¹	k_{CO}/s⁻¹	$2k_t$/dm³ mol⁻¹ s⁻¹
Hexane	670	$8.3 \cdot 10^5$	8.5×10^9
Tetradecane	620	$9.0 \cdot 10^5$	3.4×10^9
Propan-2-ol	630	$4.7 \cdot 10^5$	3.9×10^9
Ethanol	530	$5.0 \cdot 10^5$	4.4×10^9
Methanol	550	$4.2 \cdot 10^5$	6.0×10^9
Acetonitrile	620	$1.9 \cdot 10^5$	8.0×10^9

were evaluated by fits of eqns. (8)–(10) with the assumptions that the 315 nm absorption is only due to *tert*-butyl and that the quantum yield of cleavage is $\Phi = 0.72$ for all solvents.[4] For each solvent three different initial radical concentrations of typically 4.3×10^{-5}, 1.8×10^{-5} and 8.0×10^{-6} were chosen, and the corresponding traces were subjected to simultaneous fits with k_{CO}, $2k_t$ and ε_R as free parameters. The results are collected in Table 2 and have estimated errors of ±20%. In addition, kinetic traces were recorded at 230 nm for all solvents and analyzed in terms of superposition of the absorptions of *tert*-butyl and pivaloyl. This provided the absorption coefficients of *tert*-butyl and pivaloyl at 230 nm as $\varepsilon_R \approx \varepsilon_{RCO} \approx$ 2000–2500 dm³ mol⁻¹ cm⁻¹. These values are rather imprecise, however, since the lifetimes for decarbonylation and termination are similar.

Discussion

Radical Spectra.—The optical spectra obtained for benzyl and *tert*-butyl radicals agree with previous findings[8,9,30–32] except for the absorption coefficient of *tert*-butyl, $\varepsilon_{max}(317) =$ 530–670 dm³ mol⁻¹ cm⁻¹, which is larger than the earlier values $\varepsilon_{max}(307) = 200$ dm³ mol⁻¹ cm⁻¹ in 3-methylpentan-3-ol,[8] $\varepsilon_{max}(314) = 230$ dm³ mol⁻¹ cm⁻¹ in heptane[9] and $\varepsilon_{max}(333) =$ 460 dm³ mol⁻¹ cm⁻¹ in the gas phase.[31]

For pivaloyl and phenylacetyl there are no previous data. In comparison with the acetyl radical $CH_3\dot{C}O$ which has a longest wavelength band at 215 nm[33–35] with $\varepsilon_{max} = 10^4$ dm³ mol⁻¹ cm⁻¹ the pivaloyl radical exhibits similar features [$\varepsilon(230) \approx$ 2000 dm³ mol⁻¹ cm⁻¹] and does not absorb for $\lambda \geqslant 240$ nm. The absorption of phenylacetyl (Fig. 5) is red-shifted ($\lambda_{max} \approx 275$ nm) which we attribute to a conjugation between the phenyl and the carbonyl groups. In fact, AM1 calculations revealed a coplanarity of these groups in energy minimum conformations with CO in the *cis*- and *trans*-position to the phenyl ring. A similar but much stronger effect is known for the benzoyl radical which shows a broad band[36] at longer wavelength with $\varepsilon_{max}(370) = 150$ dm³ mol⁻¹ cm⁻¹.

Rate Constants.—The rate constants for self-termination of benzyl and of *tert*-butyl radicals have been studied extensively in various solvents and over wide temperature ranges in previous work and are known to be diffusion controlled.[29,37] The data obtained here (Tables 1 and 2) agree very well with the earlier findings. Moreover, for the same solvent $2k_t$ is very similar for the benzyl and the *tert*-butyl systems which supports the approximation of equal self- and cross-terminations used in the analysis.

For the decarbonylation some earlier values are also available. Thus, for phenylacetyl $k_{CO} = 6.1 \times 10^6$ and 9.1×10^6 s⁻¹ were reported for isooctane[6,7] and $k_{CO} = 5.2 \times 10^6$ s⁻¹ for methanol[6] solvent at ambient temperature. For pivaloyl they are 1.2×10^5 s⁻¹ in methylcyclopentane,[38] 3.5×10^5 s⁻¹ in toluene,[39] and 7×10^5 s⁻¹ in hexane.[11] Our data confirm that phenylacetyl decarbonylates about a factor of ten faster than pivaloyl and prove the existence of a solvent dependence which was considered insignificant before.[6] Tables 1 and 2 show that k_{CO} decreases by about a factor of four with increasing solvent polarity whereas viscosity effects are marginal.

The factors controlling the rate constant of decarbonylations have been discussed by Paul[40] who noticed that the activation energy E_{CO} decreases with increasing exothermicity ΔH of the cleavage reaction $R\text{–}\dot{C}O \rightarrow \dot{R} + CO$, and established a simple Evans–Polanyi relation between E_{CO} and ΔH. This explains why phenylacetyl reacts faster than pivaloyl: the reaction enthalpy for the former radical is about −6 kJ mol⁻¹ whereas it is about +25 kJ mol⁻¹ for the latter.[40] The solvent effect supports this view of enthalpy control. Acyl radicals $R\text{–}\dot{C}O$ are likely to have an appreciable dipole moment and will be stabilized by dipolar interactions in polar solvents whereas the product radicals and CO are non-polar [μ(CO) = 0.1 D].[41] Hence, the exothermicity of the cleavage decreases with increasing solvent polarity and the activation energy increases, correspondingly.

More quantitatively, the solvent effect can be discussed in terms of the Kirkwood's formula[42] eqn. (11), which describes

$$\ln k = \ln k_0 - \frac{1}{4\pi\varepsilon_0}\frac{N_A}{RT}\frac{\varepsilon - 1}{2\varepsilon + 1}\left(\frac{\mu_R^2}{r_R^3} - \frac{\mu_{TS}^2}{r_{TS}^3}\right) \quad (11)$$

the differences of stabilization by dipole–dipole interactions of the parent radical R and the transition state TS with the solvent medium treated as a continuum of relative permittivity (dielectric constant) ε. Here, k is the rate constant for a relative permittivity ε, k_0 its value for $\varepsilon = 1$, $\mu_{R,TS}$ are the dipole moments and $r_{R,TS}$ the radii of the radical and the transition state. Using the rate constants found for acetonitrile ($\varepsilon = 36$) and for the alkanes ($\varepsilon = 2$) eqn. (11) leads to $(\mu_R^2/r_R^3 - \mu_{TS}^4/r_{TS}^3) = 1.9 \times 10^{-30}$ A² s² m⁻¹ for the phenylacetyl and to 2.4×10^{-30} A² s² m⁻¹ for the pivaloyl case, *i.e.* a similar decrease of the stabilization during the scission for both the species. Absolute values of the dipole moments were calculated using AM1 and are $\mu_R = 8.1 \times 10^{-30}$, $\mu_{TS} = 3.7 \times 10^{-30}$ for

phenylacetyl and $\mu_R = 8.7 \times 10^{-30}$, $\mu_{TS} = 5.4 \times 10^{-30}$ A s m for pivaloyl. The radii were estimated from the molar volumes of the parent compounds phenylacetaldehyde and pivaldehyde as 320 pm for phenylacetyl and 280 pm for pivaloyl, and r_{TS} was assumed to be 20 pm larger since the calculation revealed a 50 pm elongation of R–$\dot{C}O$ bond in the transition state. These values give $(\mu_R^2/r_R^3 - \mu_{TS}^2/r_{TS}^3) = 1.7 \times 10^{-30}$ A^2 s^2 m^{-1} for phenylacetyl and 2.4×10^{-30} A^2 s^2 m^{-1} for pivaloyl. The excellent agreement with the experimental findings should not be overemphasized, however, since an application of eqn. (11) to the alcohol solvents would predict rate constants which are about two-fold lower than observed. On the other hand, deviations from eqn. (11) are common for alcohol solvents[42,43] and could be due to hydrogen bonding.

Apart from the cases reported here, the β-scission of the *tert*-butoxy radical $(CH_3)_3C\dot{O} \rightarrow (CH_3)_2CO + \dot{C}H_3$ seems the only other well documented case for a solvent dependence of a radical fragmentation rate.[44] In contrast to the acyl systems the rate constant increases substantially with increasing solvent polarity, *i.e.* the dipole moment increases on approach to the transition state. This is supported by AM1 calculations which gave $\mu_R = 6.5 \times 10^{-30}$ A s m for the *tert*-butoxy radical and a larger $\mu_{TS} = 9.2 \times 10^{-30}$ A s m. Work on this reaction is in progress.

Acknowledgements

Support of this work by the Swiss National Foundation for the Scientific Research is gratefully acknowledged. We also thank G.-H. Goudsmit for assistance in the development of the data acquisition programs.

References

1 J. C. Dalton and N. J. Turro, *Ann. Rev. Phys. Chem.*, 1970, **21**, 499.
2 P. S. Engel, *J. Am. Chem. Soc.*, 1970, **92**, 6074.
3 W. K. Robbins and R. H. Eastman, *J. Am. Chem. Soc.*, 1970, **92**, 6076.
4 N. C. Yang, E. D. Feit, N. N. Hui, N. J. Turro and J. C. Dalton, *J. Am. Chem. Soc.*, 1970, **92**, 6974.
5 H. Paul and H. Fischer, *Helv. Chim. Acta*, 1973, **56**, 1575.
6 L. Lunazzi, K. U. Ingold and J. C. Scaiano, *J. Phys. Chem.*, 1983, **87**, 529.
7 N. J. Turro, I. R. Gould and B. H. Baretz, *J. Phys. Chem.*, 1983, **87**, 531.
8 C. Huggenberger and H. Fischer, *Helv. Chem. Acta*, 1981, **64**, 338.
9 T. Chen and H. Paul, *J. Phys. Chem.*, 1985, **89**, 2765.
10 C. Arbour and G. M. Atkinson, *Chem. Phys. Lett.*, 1984, **159**, 520.
11 A. G. Neville, C. E. Brown, D. M. Rayner, J. Lusztyk and K. U. Ingold, *J. Am. Chem. Soc.*, 1991, **113**, 1869.
12 B. Blank, P. G. Mennitt and H. Fischer, *Spec. Lectures XXIII Int. Congr. Pure Appl. Chem.*, 1971, **4**, 1.
13 H. Tomkiewicz and H. Cocivera, *Chem. Phys. Lett.*, 1971, **8**, 595.
14 I. Carmichael and H. Paul, *Chem. Phys. Lett.*, 1979, **67**, 519.
15 D. D. M. Wayner and D. Griller, *Adv. Free Radical Chem.*, 1990, **1**, 169.
16 R. Hany and H. Fischer, *Chem. Phys.*, 1993, **172**, 131.
17 F. Jent and H. Paul, *Chem. Phys. Lett.*, 1989, **160**, 632.
18 C. Blättler, F. Jent and H. Paul, *Chem. Phys. Lett.*, 1990, **166**, 375.
19 G. F. Lehr and N. J. Turro, *Tetrahedron*, 1981, **37**, 3411.
20 N. J. Turro and B. Kraeutler, *Acc. Chem. Res.*, 1980, **13**, 369.
21 H. Fischer, *Chem. Phys. Lett.*, 1983, **100**, 255.
22 B. Kraeutler and N. J. Turro, *Chem. Phys. Lett.*, 1980, **70**, 270.
23 H. Fischer and H. Paul, *Acc. Chem. Res.*, 1987, **20**, 200.
24 M. Walbiner and H. Fischer, *J. Phys. Chem.*, 1993, **97**, 4880.
25 I. R. Gould, B. H. Baretz and N. J. Turro, *J. Phys. Chem.*, 1987, **91**, 925.
26 J. C. Scaiano, *J. Am. Chem. Soc.*, 1980, **102**, 7747.
27 M. B. Zimmt, C. Doubleday and N. J. Turro, *J. Am. Chem. Soc.*, 1986, **108**, 3618.
28 Y. Tanimoto, M. Takashima and M. Itoh, *Bull. Chem. Soc. Jpn.*, 1989, **62**, 3923.
29 H. Schuh and H. Fischer, *Helv. Chim. Acta*, 1978, **61**, 2130.
30 R. F. C. Claridge and H. Fischer, *J. Phys. Chem.*, 1983, **87**, 1960.
31 D. A. Parkes and C. P. Quinn, *J. Chem. Soc. Faraday Trans 1*, 1976, **72**, 1952.
32 H. R. Wendt and H. E. Hunziker, *J. Chem. Phys.*, **81**, 717.
33 H. Adachi, N. Basco and D. G. L. James, *Chem. Phys. Lett.*, 1978, **59**, 502; *Int. J. Chem. Kinet.*, 1981, **13**, 1251.
34 D. A. Parkes, *Chem. Phys. Lett.*, 1981, **77**, 527.
35 N. Basco and S. S. Parmar, *Int. J. Chem. Kinet.*, 1985, **17**, 891.
36 H. Fischer, R. Baer, R. Hany, I. Verhoolen and M. Walbiner, *J. Chem. Soc., Perkin Trans. 2*, 1990, 787.
37 H. Lehni and H. Fischer, *Int. J. Chem. Kinet.*, 1983, **15**, 733.
38 H. Schuh, E. J. Hamilton, H. Paul and H. Fischer, *Helv. Chim. Acta*, 1974, **57**, 2011.
39 J.-K. Vollenweider, H. Fischer, J. Hennig and R. Leuschner, *Chem. Phys.*, 1985, **97**, 217.
40 J.-K. Vollenweider and H. Paul, *Int. J. Chem. Kinet.*, 1986, **18**, 791.
41 A. L. McClellan, *Tables of Experimental Dipole Moments, Part 1*, Freeman, San Francisco, 1963.
42 C. Reichardt, *Solvents and Solvent Effects in Organic Chemistry*, VCH, Weinheim, 1988.
43 A. K. Salikhov and H. Fischer, *Appl. Magn. Reson.*, submitted to publication.
44 C. Walling and P. J. Wagner, *J. Am. Chem. Soc.*, 1963, **85**, 2333; 1964, **86**, 3368.
45 G. D. Mendenhall, L. C. Stewart and J. C. Scaiano, *J. Am. Chem. Soc.*, 1982, **104**, 5109.

Paper 3/07498F
Received 21*st December* 1993
Accepted 5*th January* 1994